Expanding the catalytic activity of amine dehydrogenases

Rational enzyme engineering via computational analysis and application in organic synthesis

Tseliou, V.

Publication date
2020

Document Version
Other version

License
Other

Chapter 4

Kinetic resolution of racemic primary amines using *Geobacillus stearothermophilus* amine dehydrogenase variant

Part of this chapter has been published in ChemCatChem
V. Tseliou, T. Knaus, J. Vilim, M. F. Masman, F. G. Mutti, ChemCatChem 2019, 12, 1-6
doi: 10.1002/cctc.201902085

4.1 Abstract

The high enantioselectivity of the AmDHs can be used for the preparation of valuable enantiomerically pure amines. The most well studied approach is the reductive amination of ketones. However, kinetic resolution (KR) of racemic amines can also be used for the preparation of amines with excellent optical purity. Herein, the NAD(H)-dependent engineered AmDH from *Geobacillus Stearothermophilus* LE-AmDH-v1 was applied together with NAD-oxidase from *Streptococcus mutans* (NOx) for the kinetic resolution of pharmaceutical relevant racemic a-chiral primary amines. The pH optimum for the oxidative deamination reaction was determined to be 7.4 using Britton–Robinson's universal buffer. In this pH optimum, the influence of different types of buffer was investigated for the oxidative deamination of racemic a-methylbenzylamine. Increasing the temperature of the reaction resulted in faster resolution of a-methyl-benzylamines under the optimized conditions. Pharmaceutical relevant racemic amines were successfully resolved after 24h (*ee* >99 %) using these optimized conditions. Increased concentration of a-methylbenzylamine (up to 75 mM) resulted in successful resolution using the same amount of catalyst due to the decreased inhibition of LE-AmDH-v1 compare with previously reported AmDHs. Finally, the dynamic kinetic resolution of a-methylbenzylamine was attempted using amine boranes. In all cases, only the racemic substrate was recovered indicating a possible inhibition of LE-AmDH-v1 by these complexes. Moreover, Implementation of LE-AmDH-v1 into deracemization cascades employing (*S*)-selective ω-transaminases resulted in low to moderate *ee* values.

4.2 Introduction

a-Chiral amines are fundamental building blocks for the manufacturing of many active pharmaceutical ingredients (APIs), fine chemicals, and agrochemicals.[1-4] An increasing number of newly approved drugs contain an a-chiral amine core, and the legislative regulations for their commercialisation are stringent in terms of chemical and enantiomerical purity (i.e., total impurity amount < 0.15%). In this context, several biocatalytic methods to obtain enantiopure a-chiral amines have been developed, including asymmetric synthesis from prochiral ketones using either ω-transaminases (ωTA),[5-12] or dehydrogenases (i.e., reductive aminases (RedAm), imine reductases (IRed), amine dehydrogenases(AmDH);[13-33] from alkenes using either ammonia lyases[34,35] or engineered cytochrome c;[36] and from alkanes using engineered cytochrome P411 monooxygenases.[15,37] Enantiomerically pure amines can also be obtained from a racemic mixture by applying one among several available deracemisation strategies.[38] Kinetic resolution (KR) is the simplest among these deracemisation methods, as it is based on the use of an enantioselective catalyst that acts exclusively on one enantiomer while leaving the other untouched. Additionally, KR is a practical approach to assess the efficiency of a biocatalyst that can possibly then be implemented in another deracemisation method. For instance, KR can be combined with a racemisation catalyst (i.e., dynamic KR using e.g., Pd/C, Pd/AlO(OH), $VOSO_4$, Ru or Ir complexes) or a hydride transfer reagent (e.g., $NaCNBH_3$, $NaBH_4$).[38-40] The applicability of KR and DKR for chiral amine synthesis has been demonstrated using hydrolases,[39] ωTAs,[5-7,9,10,41] and monoamine oxidases (MAOs),[42-50] as well as with AmDHs or RedAms in combination with either a NADH oxidase or an alanine dehydrogenase.[51-53]

Complementary strategies include deracemisation cascades in which stereocomplementary AmDH and ωTA, or vice versa, perform stereoselective oxidative deamination followed by stereoselective reductive amination.[54]

The KR of a-chiral amines can be performed using AmDHs in combination with a H_2O-forming NADH oxidase (NOx), thereby maximising the atom-economy, as

dioxygen acts as an oxidant and water is the by-product. However, the restricted substrate scope of AmDHs imposes a limitation on the applicability of the AmDH-NOx system, as most of the currently available AmDHs were engineered starting from structurally related wild-type enzymes and using a similar engineering approach. However, we recently reported a highly stereoselective AmDH (LE-AmDH-v1), which was engineered starting from a wild-type enzyme that does not catalyse any apparent asymmetric transformation in its natural reaction, namely the ε-deaminating L-lysine dehydrogenase (LysEDH) from *Geobacillus stearothermophilus*[27] LE-AmDH-v1 exhibited excellent activity and stereoselectivity in the asymmetric synthesis of pharmaceutically relevant (*R*)-configured α-chiral amines, including (*R*)-α-methylbenzylamines, (*R*)-1-aminotetraline, and (*R*)-4-aminochromane. Notably, the previously discovered AmDHs do not possess this property.[13,15,23-33] Herein, we report the harnessing of the catalytic and stereoselective properties of LE-AmDH-v1 to carry out the KR (i.e., enantioselective oxidative deamination) of pharmaceutically relevant α-chiral amines starting from a racemic mixture of α-methyl- and α-ethyl-benzylamines, 1-aminotetralin, 4-aminochromane, and 1-aminoindan.

4.3 Results and discussion

4.3.1 Response factors

For an accurate determination of the obtained conversions of the racemic amines into the corresponding ketones, we determined the response factors of amines **1-7a** and ketones **1-7b** by comparing the corresponding GC peak areas at different concentrations of analyte (**Table 1**). Using the obtained slopes the conversion of the KR of a racemic compound into its corresponding ketone was determined as described in methods section (section 4.5.2).

Table 1. Response factors of the substrates and products used.

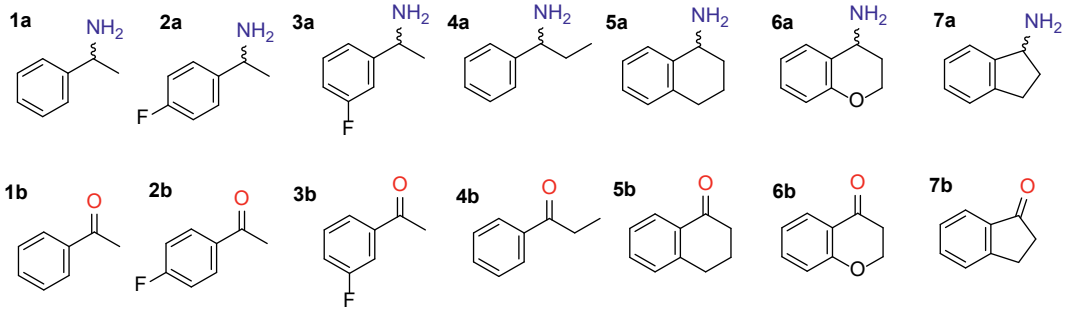

Entry	DMSO stock	Conc. (mM)	Area extracted of		Slope (R^2)		Response factor	
			1a	**1b**	**1a**	**1b**	**1a/1b**	**1b/1a**
1	1 M	5	504	626	104.87 (0.99)	111.99 (0.99)	0.94	1.06
		7.5	739	884				
		10	1047	1075				
		15	1553	1592				
		20	2136	2295				
			2a	**2b**	**2a**	**2b**	**2a/2b**	**2b/2a**
2	1 M	5	715	814	140.51 (0.99)	151.45 (0.99)	0.93	1.08
		7.5	994	1138				
		10	1459	1572				
		15	2105	2267				
		20	2805	2989				
			3a	**3b**	**3a**	**3b**	**3a/3b**	**3b/3a**
3	1 M	5	437	396	104.14 (0.98)	117.89 (0.95)	0.88	1.13
		7.5	657	587				

Entry	DMSO stock	Conc. (mM)	Area extracted of		Slope (R^2)		Response factor	
		10	852	770				
		15	1285	1187				
		20	1523	1434				
			4a	**4b**	**4a**	**4b**	**4a/4b**	**4b/4a**
		5	606	569				
		7.5	899	851				
4	1 M	10	1202	1102	123.51 (0.99)	114.63 (0.99)	1.08	0.93
		15	1840	1715				
		20	2510	2323				
			5a	**5b**	**5a**	**5b**	**5a/5b**	**5b/5a**
		5	398	532				
		7.5	628	766				
5	1 M	10	831	978	84.51 (0.99)	98.37 (0.99)	0.86	1.16
		15	1288	1495				
		20		1935				
			6a	**6b**	**6a**	**6b**	**6a/6b**	**6b/6a**
		5	463	371				
		7.5	666	540				
6	1 M	10	849	665	88.65 (0.99)	68.93 (0.99)	1.28	0.78
		15	1370	1075				
		20	1756	1344				
			7a	**7b**	**7a**	**7b**	**7a/7b**	**7b/7a**
		5	593	540				
		10	1307	1168				
7	1 M	15	1811	1632	123.8 (0.99)	110.97 (0.99)	1.08	0.93
		20	2449	2205				
		25	3122	2785				

4.3.2 Influence of the pH in the oxidative deamination of α-methyl-benzylamine

Initially, we determined the optimum pH for the biocatalytic oxidation using **1a** as substrate. The rate of the oxidative deamination reaction of **1a** (10 mM) was investigated in a pH range from 2.5 to 9.8 using Britton–Robinson's universal buffer using LE-AmDH-v1 (45 μM), NAD^+ (1 mM) and NAD-oxidase (NOx, 3 μM) from

Streptococcus mutans for cofactor recycling (**Figure 1A**). The study was performed at 40 °C due to the reported thermal stability of NOx that is limited up to 52 °C. Conversely, we have previously demonstrated that LE-AmDH-v1 is a thermostable enzyme (T_m: 69 °C). **Figure 1** shows that the reaction rate was the highest at pH 7.4 (56.2 μM/min). Although, we have previously shown that LE-AmDH-v1 better performed the reductive amination at pH 9-9.5, in the oxidative deamination direction, more basic pH reduced the reaction's rate. For instance, at pH 9.2 the rate of the reaction was determined to be 34.6 μM min^{-1} or 18.3 μM min^{-1} at pH 9.7, respectively.

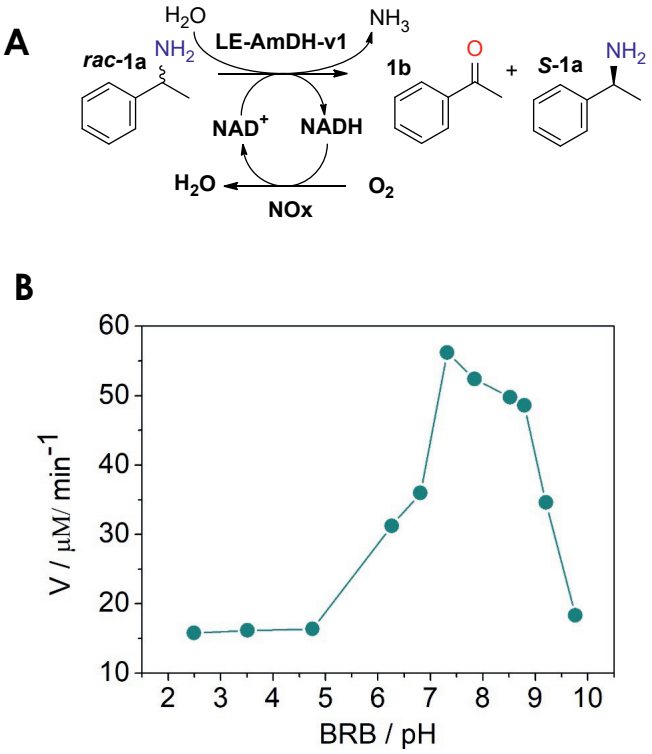

Figure 1. (A) Schematic representation of the reactions performed. (B) Reaction rate of the oxidative deamination of *rac*-1a at different pH values using Britton–Robinson's universal buffer. Catalytic amount of NAD^+ (1mM) was applied and recycled using the NOx (3 μM). All reactions (0.5 mL) were performed at 40 °C using 10 mM of **1a** and 45 μM of LE-AmDH-v1. Reaction times varied from 5 to 40 min.

4.3.3 Influence of the type of buffer

Next, we investigated the influence of different types of buffer for the oxidative deamination of **1a** (10 mM) catalyzed by LE-AmDH-v1 (45 μM) in presence of NOx (3μM). The temperature was reduced to 30 °C to avoid any evaporation of the product at longer reaction times as was partially observed in the previous set of experiments. Conversion and *ee* values obtained were acquired for the KR at the optimum pH of 7.4 in 50 mM Tris-HCl, 100 mM KPi, 100 mM MOPS and 100 mM HEPES buffers. Results are summarized in **Figure 2**. In general, biocatalytic transformations proceeded equally well and reached the highest conversion of 48 % and 49% after 24 h in 50 mM Tris/HCl and 100 mM KPi buffers, respectively. In both cases the reaction reached completion after this time as *ee* was more than 99% for the (*S*)-configured product. A more detailed study showed that enantiopure (*S*)-**1a** was obtained after 16 h using both buffers, thus indicating that prolonging the reaction time is unnecessary. In contrast, the LE-AmDH-v1 performed less efficiently in 100 mM MOPS buffer; a maximum conversion of only 35% was obtained after 24 h (*ee* = 57% *S*). A similar scenario was observed when using a HEPES buffer (100 mM pH 7.4), which provided a maximum conversion of 36% (ee = 61% S) after 24 h.

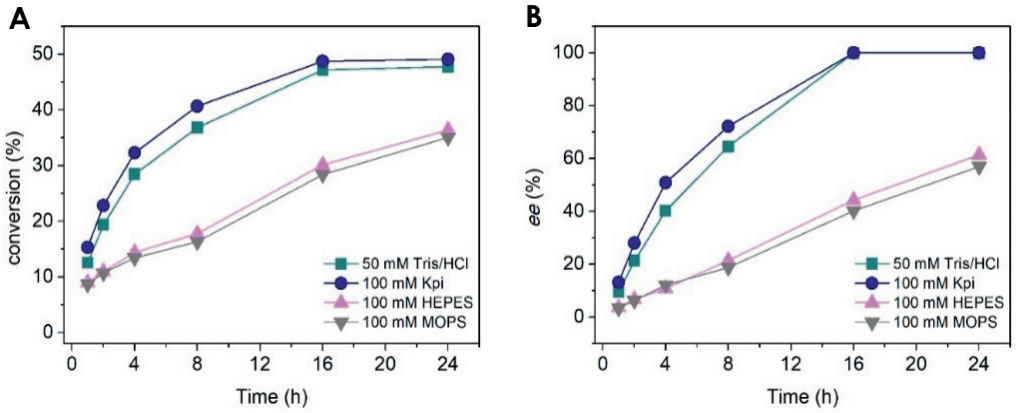

Figure 2. KR of *rac*-1a (10 mM) catalyzed by LE-AmDH-v1 (45 μM) and using different types of buffers with NAD+ (1 mM) and NOx (3 μM) at 30 °C. (A) Progress of the KR over the time. (B) Variation of the ee of the unreacted enantiomer over the time.

4.3.4 Influence of the temperature into the stereoselective outcome

With the aim of investigating the influence of the temperature on the oxidative KR of **1a**, we monitored the progress of enantiomeric excess at different temperatures (30 °C, 40 °C and 50 °C). Reactions were performed in 50 mM Tris/HCl pH 7.4 comprising LE-AmDH-v1 (90 μM), NOx (10 μM), and analyzed after 2h, 4h, 8h, 16h and 24h. **Figure 3** shows that complete KR of **1a** (*ee* >99% *S*) was obtained after 16h at 30 °C or 40 °C. However, the KR proceeded at higher rate at 40 °C as the *ee* reached already 99.1% after 8 h, whereas it was 95.2% at 30 °C after the same time. At 50 °C, the KR proceed even faster and only (*S*)-**1a** remained in the reaction mixture after 8 h. However, due to the reported mesophilic thermal stability of NOx (Tm 52 °C), we decided to attempt the KR of *rac*-**2-7a** at 30 °C (**Table 2**) and eventually to increase the temperature only in those cases in which resolution would not reach completion at 30 °C within 24 h.

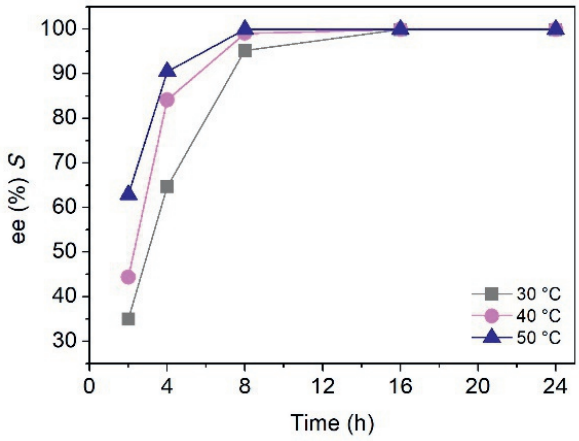

Figure 3. Progress of the KR of *rac*-1a (10 mM) at different temperatures (30 °C- 50 °C) catalyzed by LE-AmDH-v1 (90 μM) with NAD+ (1 mM) and NOx (10 μM).

4.3.5 Kinetic resolution of pharmaceutical relevant *racemic* amines employing LE-AmDH-v1

On the basis of the investigation performed for compound **1a**, the LE-AmDH-v1 was applied for the kinetic resolution of racemic amines **2**-**6a**. Normalized conversions using the response factors (**Table 1**) as well as the *ee* of the obtained amines are reported in **Table 2**. In all cases, the production of enantiopure amines was achieved by the biocatalytic kinetic resolution using LE-AmDH-v1 under the reported conditions with the exception of fluoro substituted a-methylbenzylamines. Starting from these racemic amines, the *ee* values of **2a** and **3a** were respectively 94% and 77% (*S*), thus indicating that the reaction did not reach completion at 30 °C after 24 h. Longer reaction times (48 h) allowed the KR to reach completion in the case of **2a** (*ee*: >99%), whereas **3a** was obtained in higher enantioenriched form (*ee*: 95%). The same results were observed when *rac*-**2a** and *rac*-**3a** were resolved at 50 °C for 24 h, thereby affording ee values of >99% and 95%, respectively. These results indicate that higher temperatures can indeed accelerate the kinetics of the reaction, as previously reported for reductive amination of ketones catalyzed by

LE-AmDH-v1. Finally, LE-AmDH-v1 was able to resolve **5-7a** at 30 °C after 24 h; these bicyclic aromatic enantiopure amines are motives in many important pharmaceuticals, such as Rotigotine (a dopamine agonist), Norsertraline (a selective serotonin reuptake inhibitor, SSRI), and Resagiline (an irreversible inhibitor of monoamine oxidase-B).

Table 2. Kinetic resolution of racemic amines 1-7a employing LE-AmDH-v1. Reaction conditions: [substrate]: 10 mM, [NAD^+]: 1 mM, [LE-AmDH-v1]: 90 µM, [NOx]: 10 µM, Temperature: 30 °C, Time: 24h

Substrate	Time (h)	Conv. (%)[a]	*ee* [c]
1a	24	49.84	>99.3 % (*S*)
2a [b]	48	49.72	>99.2 % (*S*)
3a [b]	48	46.12	94.9 % (*S*)
4a	24	50.37	>99.4 % (*S*)
5a	24	49.44	>99.5 % (*S*)
6a	24	49.86	>99.3 % (*S*)
7a	24	50.40	>99.6 % (*S*)

[a] conversion reported here are normalized based on the response factors of the obtained amines: ketones as describe in the **Table 1**.

[b] reaction time: 48h.

[c] In some analytical scale reactions, it was possible to determine the *ee* values with an accuracy superior to 99.2 % due to the elevated conversion and the high response GC factor of the amine product. In these cases, the (*R*)-enantiomer was never observed.

4.3.6 Influence of the substrate concentration in the kinetic resolution of a-methyl-benzylamine

In a previous work by Yun's group the kinetic resolution of *rac* **1a** was attempted using the cFL1-AmDH that was previously engineered by Bommarius and co-workers.[25] However, due to significant inhibitory effect of **1a** in the activity of cFL1-AmDH as we have previously demonstrated,[27] the authors had to use a large amount of whole cells (100 mg_{DCW} mL^{-1}) co-expressing cFL1-AmDH and an NADH oxidase (NOx) *Lactobacillus brevis*[55] in order to resolve 20 mM of **1a**. We have previously determined that LE-AmDH-v1 possess 20-fold reduced IC_{50} and 38-fold reduced K_I values for **1a** as inhibitor compare with cFL1-AmDH; therefore we investigated the kinetic resolution of **1a** at higher substrate concentrations

while keeping constant the amount of LE-AmDH-v1 present in the reaction mixture (90 μM). **Figure 4** shows that 90 μM of LE-AmDH-v1 were sufficient for resolving 50 mM of *rac*-**1a** after 24 h, leading to enantiopure (*S*)-**1a** (conv. 50%) at 30 °C. Elevated *ee* (95% S) and conversion into **1b** (48%) were also obtained at 75mM of **1a**, while KR was not effective at 100 mM of the same substrate (*ee*: 11% *S*) with the conversion into the corresponding ketone to be 14%. Increasing the temperature to 40 °C resulted in full resolution of 75 mM of *rac*-**1a** after 24 h using the same amount of LE-AmDH-v1. The resolution of 100 mM of *rac*-**1a** was also improved by increasing the temperature from 30 °C to 40 °C as the conversion increased from 14% to 57%.

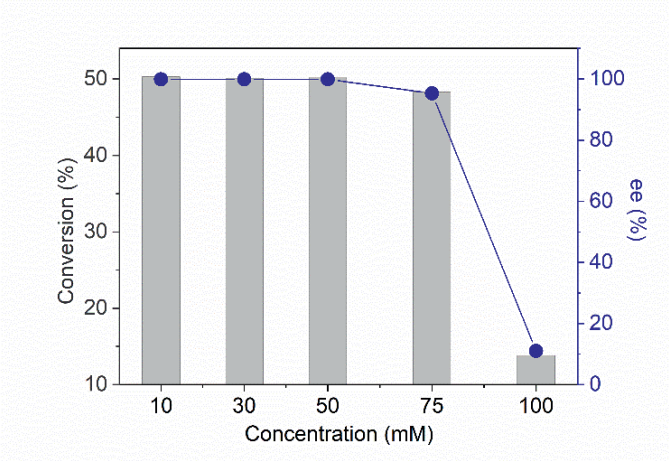

Figure 3. Investigation on the influence of the substrate concentration in the oxidative kinetic resolution of 1a. Reactions were performed at 30 °C using 10 mM of **1a**, 1 mM of NAD^+, 90 μM of LE-AmDH-v1 and 10 μM of NOx.

4.3.7 Kinetic resolution in semi-preparative scale.

Finally, the potential usefulness of the LE-AmDH-v1/ NOx system was tested in semi-preparative scale amination starting from 100 mg of *rac*-**1a** (50mM). After 24h, the KR reached completion and resulted in 49.81% conversion into the corresponding ketone **1b**. The ketone formed was removed by extraction with

MTBE under acidic conditions. After basification, the (*S*)-**1a** was obtained with 43.6% isolated yield (theoretical maximum is 50%) and with 99.2% *ee*.

4.3.8 Dynamic kinetic resolution of α-methyl-benzylamine using amine boranes

In this set of reactions, we applied the LE-AmDH-v1 for the DKR of **1a** by using H_3NBH_3 as a racemization catalyst. Starting either from 10 mM or 50 mM of *rac*-**1a** and by adding 4 or 8 eq., of H_3NBH_3 in the reaction mixture we observed no conversion into the corresponding ketone (**1b**). In fact, the amine **1b** was obtained in racemic form (*ee*: 0.8% *S*) indicating no activity by LE-AmDH-v1 at all, possibly due to inhibitory effects of ammonia borane into the activity of LE-AmDH as previously reported for berberine bridge enzyme.[3] As last attempt, we followed a sequential one-pot, two-step procedure in which the KR of **1a** was performed using the optimized process for 24h to yield (*S*)-**1b** (50% conv., >99% *ee*), following by addition of 8 eq. NH_3-BH_3 for another 24h as described in the methods. After that time only **1a** was present in the reaction mixture which was obtained in enantiopure (*S*)-configuration (*ee* >99%). However, analysis of the reaction mixture revealed the ammonia borane complex reduced the remaining ketone to alcohol indicating that the second step was unsuccessful. Incubation of 25 mM **1b** in Tris-HCl pH 7.4 with 4 or 10 equivalents of ammonia borane for 1 h at 30 °C resulted in alcohol formation indicating that the alcohol observed, was formed from the reduction of the remaining ketone by the ammonia-borane after the first 24 h. In another study,[1] more bulky or less water soluble boranes (e.g. morpholine-BH_3 or Me_3N-BH_3) found to also compatible with enzymes employed in deracemization cascades. Therefore we also tested 4 or 8 eq of morpholine borane for the DKR of 50 mM *rac*-**1a**. In both cases the reaction proceeded with 0-10 % *ee* for the (*S*)-configured **1a**. As always, the positive control (without addition of morpholine borane complex) resulted in >99% for (*S*)-**1a** after the reaction time indicating that morpholine borane has a negative effect in the activity of LE-AmDH-v1.

4.3.9 Biocatalytic deracemization cascades employing LE-AmDH-v1 and (*S*)-selective ω-TAs

Finally we employed the *R* selective LE-AmDH-v1 together with the (*S*)-selective *Vf*-ωTA originated from *Vibrio fluvialis*[4] in the deracemization cascades shown in **scheme 1**. The first cascade requires LDH for cofactor recycling while transforming the pyruvate produced by the ω-TA to L-lactate (**Scheme 1A**). Similarly in the second cascade (**Scheme 1B**), Ala-DH recycles the cofactor while converting the produced pyruvate to L-alanine which is required by the ω-TA. Since *Vf*-ωTA is (*S*)-selective, the remaining 50 % ketone will be converted to the (*S*)-configured amine. These enzymatic cascades were performed using 90 μM of AmDH and 50 μM of ω-TA at substrate concentrations of 25 or 50 mM. After the reported times (see Methods 4.5.5) the reaction mixture of the first cascade contained 19 % or 16 % of the ketone starting from 25 or 50 mM *rac*-**1a**, respectively, while the amine was obtained with 28% or 15% ee for the (*S*)-configured **1a**. A similar scenario was observed with the second case. Starting from 50 mM of *rac*-**1a** the one-pot system proceeded with 15% conversion into **1b**. Analysis of the stereoselective outcome of the cascade revealed the **1a** was obtained in nearly racemic form (*ee* 3% *R*).

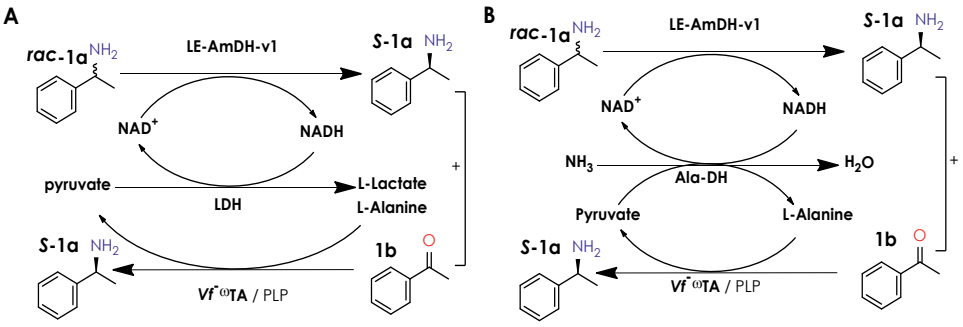

Scheme 1. Enzymatic cascades applied for the deracemization of 1a. (A) Reaction conditions: [substrate]: 25 or 50 mM, [NAD^+]: 1 mM, [PLP]: 1 mM [LE-AmDH-v1]: 90 μM, [Vf-ωTA]: 50 μM. [LDH]: 1 mg mL^{-1}, 100 mM Tris-HCl pH 7.3 supplemented with 5 eq. L-alanine, Temperature: 30 °C, Time: 24 h. (B) Reaction conditions: [substrate]: 50 mM, [NAD^+]: 1 mM, [PLP]: 1 mM [LE-AmDH-v1]: 90 μM, [Vf-ωTA]: 50 μM. [Ala-DH]: 20 μM, 100 mM KPi pH 7.3 supplemented with 150 mM L-alanine and 100 mM $HCOONH_4$, Temperature: 30 °C, Time: 24 h.

4.4 Conclusions

In summary, we have applied the recently engineered LE-AmDH-v1 for the kinetic resolution of a selection of substrates that proved to be challenging for the other available AmDHs so far. For instance, only low activities were observed for the reductive amination of **5b** using *Bb*-AmDH, cFL1-AmDH and *Cal*-AmDH[24,25,28] while no activity towards **6b** or **7b** was reported with any of the AmDHs developed up to date. Similarly, cFL1-AmDH performed the reductive amination of respective ketones **1**-**4b** yielding from poor to moderate conversion after 48 h,[56] and low activity was observed with *Es*-LeuDH (AmDH) for the reductive amination of **1b** and **4b**.[31] In the oxidative deamination direction (KR), only few α-methylbenzylamines could be resolved but at the expense of a large amount of whole cells biocatalysts,[51] and by using a less atom-efficient pyruvate/AlaDH system for NAD^+ recycling.[52] Herein, we used the LE-AmDH-v1/NOx system to access pharmaceutically relevant optically active amines in (*S*)-configuration starting from the respective racemic mixtures. The oxidative kinetic resolution proceeded efficiently at the optimum pH of 7.4 in 50 mM Tris-HCl or 100 mM KPi. At 30 °C the KR reached completion after 16 h and the increase of the reaction temperature from 30 °C to 50 °C resulted in the resolution of **1a** within 8 h. Using these optimal conditions the kinetic resolution of α-methylbenzylamines, 1-aminotetralin, 1-aminoindan and 4-aminochroman was complete in all cases with the exception of **3a** which proceeded with 95% ee after 48 h. LE-AmDH-v1 could not be combined with any chemical reducing agent (ammonia borane or morpholine borane) to achieve quantitative yield most possibly due to inhibition of the biocatalyst with these amine borane complexes. In addition, application of LE-AmDH-v1 with the (*S*)-selective ω-transaminase *Vf*-ωTA in deracemization cascades resulted in amine product with low ee.

4.5 Methods

4.5.1 General procedure for biocatalytic oxidative kinetic resolution

Biotransformations were performed in 1.5 mL Eppendorf tubes with a total reaction volume of 0.5 mL. The optimized reaction consisted of NAD^+ (1 mM), substrate (10 mM), LE-Am-DHv1 (90 µM) and NOx (10 µM). Reactions were performed at 30 °C for 24 h on orbital shakers (170 rpm) in a horizontal position. The reactions were quenched after 24 h by the addition of aqueous KOH (10 M, 100 µL), the organic compounds were extracted with dichloromethane or ethyl-acetate (2 x 550 µL), dried with magnesium sulfate and the conversions were measured by GC-FID.

4.5.2 Determination of response factors and calculation of final conversions

The Response factors of amines **1-7a** and ketones **1-7b** were determined by GC-FID by comparing the corresponding GC peak areas of amine and ketones at different concentrations of analyte. For a given final concentration (e.g., 5 mM) both the amine and its corresponding ketone (e.g., **1a** and **1b**) were pipetted into the same reaction tube containing the reaction buffer (1 mL, 50 mM Tris-HCl pH 7.34) and incubated at 25 °C for 1 h. After that the mixture was basified with 100 µL of 10 M KOH and split into equal volumes (2 x 500 µL). Each aliquot was extracted with 550 µL of dichloromethane. The organic phases were combined, dried over $MgSO_4$ and analyzed by GC-FID. The obtained areas were plotted against the concentration used. The response factors were calculated by divided the obtained slopes (**Table 1**). Conversions of racemic amines into the corresponding ketones were finally normalized using the response factor of amine:ketone. For instance, the KR of a-chromamine resulted in 43.73 % conversion to a-chromanone. The response factor of a-chromanine to a-chromanone was determined to be 1.28. Multiplying the initial conversion of ketone with the response factor (amine: ketone) resulted in 56.24% as normalized conversion into a-chromanone. The final conversion was calculated by dividing this normalized conversion with the sum of the amine left in the reaction mixture

(%) and the normalized conversion of the ketone (%). The resulted number was multiplied by 100.

4.5.3 pH study for the oxidative kinetic resolution of 1a catalyzed by LE-AmDH-v1

Biocatalytic reactions were performed for different times (0-40 min). In all cases, only data points for which the conversion was below 20 % were considered in order to ensure that the reaction rate was always in the linear range. The product produced (mM) at different times was calculated based on the conversions and plotted versus the time. The velocity of the reaction (μM min^{-1}) was calculated from the obtained slope. Reactions were performed with 10 mM of substrate, 1 mM NAD^+, 45 μM of LE-AmDH-v1 and 3 μM of NOx, in Britton–Robinson's universal buffer (pH 2.5-9.2, 0.5 mL final volume).

4.5.4 Dynamic kinetic resolution using amine boranes

The DKR reactions were performed in 1.5 mL Eppendorf tubes with a total reaction volume of 0.5 mL. The reaction buffer Tris-HCl (50 mM pH 7.3) consisted of NAD^+ (1 mM), substrate (50 mM, 3.029 mg, 0.025 mmol), LE-Am-DH-v1 (90 μM) and NOx (10 μM). In the cases of the two-step one-pot reactions, the reactions were performed at 30 °C for 24 h on orbital shakers (170 rpm) to allow kinetic resolution to reach completion. After that time, the ammonia borane complex was added (4 eq., 3.087 mg, 1 mmol or 8 eq., 6.174 mg, 2 mmol) and the reaction was run for another 24 h. For the reaction with morpholine borane, 10.1 mg (4 eq.) or 20.2 mg (8 eq.) were added into the reaction mixture (0.5 mL, 50 mM of substrate) and the reactions were run for 24 h. The amine borane complexes were quenched by the addition of concentrated HCl (~ 300 μL) and after basification with 10 M KOH (pH >10) the reaction mixture was extracted with ethyl acetate (2 x 500 μL).

4.5.5 Biocatalytic deracemization cascades employing LE-AmDH-v1 and S selective ω-TAs

For the deracemization cascade shown in **scheme 1A**, reactions of 1 mL consisted of 100 mM Tris-HCl buffer pH 7.3 supplemented with NAD^+ (1 mM), PLP

(0.5 mM), L-alanine 150 mM and *rac*-**1a** (25 or 50 mM). The (*S*)-selective *Vf*-ωTA (50 μM), and the *R* selective LE-AmDH-v1 were added together with LDH (1 mg mL^{-1}) and the reactions were run at 30 °C for 24 h on orbital shakers (170 rpm) in a horizontal position. For the deracemization cascade shown in **scheme 1B** reactions of 1 mL consisted of 100 mM KPi buffer pH 7.3 supplemented with $HCOONH_4$ (100 mM), L-alanine (150 mM), NAD^+ (1 mM) and PLP (0.5 mM). *Vf*-ωTA and LE-AmDH-v1 were added at the final concentrations of 50 μM and 90 μM, respectively. Finally, Ala-DH (20 μM) was added and the reactions were run at 30 °C for 24 h on orbital shakers (170 rpm) in a horizontal position. The organic compounds were extracted with dichloromethane or ethyl-acetate (2 x 500 μL), dried with magnesium sulfate and the conversions were measured by GC-FID.

4.5.6 Analytical methods for the determination of conversions and of the absolute configurations

The conversions for the enantioselective oxidative deamination (KR) were determined by GC using a 7890A GC system (Agilent Technologies), equipped with a FID detector using H_2 as carrier gas and a DB-1701 column from Agilent (30 m, 250 μm, 0.25 μm). The following method was used: constant pressure 6.9 psi, split ratio 40:1, T injector 250 °C. Temperature Program: T initial 60 °C, hold 6.5 min, gradient 20 °C/min up to 100 °C; hold 1 min, gradient 20 °C/min up to 280 °C; hold 1 min.

After the extraction of the obtained amines, a solution of DMAP (50 mg) in 1 mL of acetic anhydride was prepared. In total, 50 μL of this solution were added to the organic phase containing 25 mM of the obtained amine(*i.e.* for reactions with 50 mM of *rac* amine substrate). The mixtures were shaken at 25 °C for 30 min. After that, 500 μL of water was added and shaken for another 30 min at 25 °C. The samples were centrifuged for 10 min at 14.800 rpm and the organic phases were dried with magnesium sulfate prior to injection in a Chrompack Chiracel Dex-CB column (length 25 m, internal diameter 0.32 mm). The following method was used: constant Flow: 1.4 mL/min, split ratio 40:1, T injector 200 °C. Temperature Program: T initial 100 °C, hold 2 min, gradient 1°C/min up to 130 °C;

hold 5 min, gradient 10 °C/min up to 170 °C; hold 10 min, gradient 10 °C/min up to 180 °C; hold 1 min

4.5.7 Dynamic kinetic resolution in semi-preparative scale

Preparative scale reactions of 1a (50 mM, 100 mg, 0.825 mmol) was performed in a total volume of 16.5 mL of Tris-HCl buffer (50 mM, pH 7.4) at 30 °C. The reaction mixture contained LE-AmDH-v1 (90 μM, 4 mg mL^{-1}), NOx (10 μM, 0.5 mg mL^{-1}), NAD^+ (1 mM). After 24 h, a 49.81% conversion was obtained for **1b**. The reaction was acidified with concentrated HCl (~1 mL) the ketone formed was extracted with MTBE (2 x 20 mL). After the addition of KOH (10 M, ~1 mL), the amine products were extracted with MTBE (3 x 20 mL). The combined organic layers were dried over $MgSO_4$ and concentrated under reduced pressure. Avoiding any further purification step, (*S*)-**1b** was obtained with 43.6% isolated yield (colorless liquid, 43.1mg, 0.356 mmol) and with 99.2% *ee*.

4.6 References

1 Wittcoff, H. A., Rueben, B. G. & Plotkin, J. S. *Industrial Organic Chemicals, 2nd ed.*, (Wiley-Interscience, New York, 2004).

2 Ghislieri, D. & Turner, N. J. *Top. Catal.* **57**, 284-300, doi:10.1007/s11244-013-0184-1 (2013).

3 Constable, D. J. C. *et al. Green Chem.* **9**, 411-420, doi:10.1039/b703488c (2007).

4 Nugent, T. C. *Chiral amine synthesis: Methods, Developments and Applications*. (Wiley-VCH, 2010).

5 Slabu, I., Galman, J. L., Lloyd, R. C. & Turner, N. J. *ACS Catal.* **7**, 8263-8284, doi:10.1021/acscatal.7b02686 (2017).

6 Guo, F. & Berglund, P. *Green Chem.* **19**, 333-360, doi:10.1039/c6gc02328b (2017).

7 Kelly, S. A. *et al. Chem. Rev.* **118**, 349-367, doi:10.1021/acs.chemrev.7b00437 (2018).

8 Gomm, A. & O'Reilly, E. *Curr. Opin. Chem. Biol.* **43**, 106-112, doi:10.1016/j.cbpa.2017.12.007 (2018).

9 D. Patil, M., Grogan, G., Bommarius, A. & Yun, H. *Catalysts* **8**, 254, doi:10.3390/catal8070254 (2018).

10 Fuchs, M., Farnberger, J. E. & Kroutil, W. *Eur. J. Org. Chem.*, 6965-6982, doi:10.1002/ejoc.201500852 (2015).

11 Savile, C. K. *et al. Science* **329**, 305-309, doi:10.1126/science.1188934 (2010).

12 Pavlidis, I. V. *et al. Nat. Chem.* **8**, 1076-1082, doi:10.1038/nchem.2578 (2016).

13 Sharma, M., Mangas-Sanchez, J., Turner, N. J. & Grogan, G. *Adv. Synth. Catal.* **359**, 2011-2025, doi:10.1002/adsc.201700356 (2017).

14 Mangas-Sanchez, J. *et al. Curr. Opin. Chem. Biol.* **37**, 19-25, doi:10.1016/j.cbpa.2016.11.022 (2017).

15 Patil, M. D., Grogan, G., Bommarius, A. & Yun, H. *ACS Catal.*, 10985-11015, doi:10.1021/acscatal.8b02924 (2018).

16 Dong, J. *et al. Angew. Chem. Int. Ed.* **57**, 9238-9261, doi:10.1002/anie.201800343 (2018).

17 Aleku, G. A. *et al. Nat. Chem.*, **10**, 961-967, doi:10.1038/nchem.2782 (2017).

18 Wetzl, D. *et al. ChemCatChem* **8**, 2023-2026, doi:10.1002/cctc.201600384 (2016).

19 Scheller, P. N., Lenz, M., Hammer, S. C., Hauer, B. & Nestl, B. M. *ChemCatChem* **7**, 3239-3242, doi:10.1002/cctc.201500764 (2015).

20 Roiban, G.-D. *et al. ChemCatChem* **9**, 4475-4479, doi:10.1002/cctc.201701379 (2017).
21 Schober, M. *et al. Nat. Catal.* **2**, 909-915, doi:10.1038/s41929-019-0341-4 (2019).
22 Matzel, P., Gand, M. & Höhne, M. *Green Chem.* **19**, 385-389, doi:10.1039/c6gc03023h (2017).
23 Abrahamson, M. J., Vazquez-Figueroa, E., Woodall, N. B., Moore, J. C. & Bommarius, A. S. *Angew. Chem. Int. Ed.* **51**, 3969-3972, doi:10.1002/anie.201107813 (2012).
24 Abrahamson, M. J., Wong, J. W. & Bommarius, A. S. *Adv. Synth. Catal.* **355**, 1780-1786, doi:10.1002/adsc.201201030 (2013).
25 Bommarius, B. R., Schurmann, M. & Bommarius, A. S. *Chem. Commun.* **50**, 14953-14955, doi:10.1039/c4cc06527a (2014).
26 Knaus, T., Böhmer, W. & Mutti, F. G. *Green Chem.* **19**, 453-463, doi:10.1039/c6gc01987k (2017).
27 Tseliou, V., Knaus, T., Masman, M. F., Corrado, M. L. & Mutti, F. G. *Nat. Commun.* **10**, 3717, doi:10.1038/s41467-019-11509-x (2019).
28 Pushpanath, A., Siirola, E., Bornadel, A., Woodlock, D. & Schell, U. *ACS Catal.* **7**, 3204-3209, doi:10.1021/acscatal.7b00516 (2017).
29 Chen, F.-F. *et al. ACS Catal.* **8**, 2622-2628, doi:10.1021/acscatal.7b04135 (2018).
30 Ye, L. J. *et al. ACS Catal.* **5**, 1119-1122, doi:10.1021/cs501906r (2015).
31 Lowe, J., Ingram, A. A. & Groger, H. *Bioorg. Med. Chem.* **26**, 1387-1392, doi:10.1016/j.bmc.2017.12.005 (2018).
32 Mayol, O. *et al. Nat. Catal.* **2**, 324-333, doi:10.1038/s41929-019-0249-z (2019).
33 Mayol, O. *et al. Catal. Sci. Technol.* **6**, 7421-7428, doi:10.1039/c6cy01625a (2016).
34 Bartsch, S. & Vogel, A. in *Science of Synthesis, Biocatalysis in Organic Synthesis 2, Chapter 2.3.3 Addition of Ammonia and Amines to C=C Bonds* (eds K. Faber, W.-D. Fessner, & N. J. Turner) 291-311 (Georg Thieme Verlag KG, 2015).
35 Li, R. *et al. Nat. Chem. Biol.* **14**, 664-670, doi:10.1038/s41589-018-0053-0 (2018).
36 Cho, I. *et al. Angew. Chem. Int. Ed.* **58**, 3138-3142, doi:10.1002/anie.201812968 (2019).
37 Prier, C. K., Zhang, R. K., Buller, A. R., Brinkmann-Chen, S. & Arnold, F. H. *Nat. Chem.* **9**, 629-634, doi:10.1038/nchem.2783 (2017).
38 Musa, M. M., Hollmann, F. & Mutti, F. G. *Catal. Sci. Technol.* **9**, 5487-5503, doi:10.1039/c9cy01539f (2019).

39 Verho, O. & Backvall, J. E. *J. Am. Chem. Soc.* **137**, 3996-4009, doi:10.1021/jacs.5b01031 (2015).

40 Schrittwieser, J. H., Velikogne, S., Hall, M. & Kroutil, W. *Chem. Rev.* **118**, 270-348, doi:10.1021/acs.chemrev.7b00033 (2018).

41 Shin, J.-S. & Kim, B.-G. *Biotechnol. Bioeng.* **60**, 534-540, doi:10.1002/(sici)1097-0290(19981205)60:5<534::aid-bit3>3.0.co;2-l (1998).

42 Turner, N. J. *Curr. Opin. Chem. Biol.* **14**, 115-121, doi:10.1016/j.cbpa.2009.11.027 (2010).

43 Dunsmore, C. J., Carr, R., Fleming, T. & Turner, N. J. *J. Am. Chem. Soc.* **128**, 2224-2225, doi:10.1021/ja058536d (2006).

44 Ghislieri, D. *et al. J. Am. Chem. Soc.* **135**, 10863-10869, doi:10.1021/ja4051235 (2013).

45 Yasukawa, K., Nakano, S. & Asano, Y. *Angew. Chem. Int. Ed.* **53**, 4428-4431, doi:10.1002/anie.201308812 (2014).

46 Heath, R. S., Pontini, M., Bechi, B. & Turner, N. J. *ChemCatChem* **6**, 996-1002, doi:10.1002/cctc.201301008 (2014).

47 Li, G. *et al. ACS Catal.* **4**, 903-908, doi:10.1021/cs401065n (2014).

48 Leisch, H., Grosse, S., Iwaki, H., Hasegawa, Y. & Lau, P. C. K. *Can. J. Chem.* **90**, 39-45, doi:10.1139/v11-086 (2012).

49 Herter, S. *et al. Bioorg. Med. Chem.* **26**, 1338-1346, doi:10.1016/j.bmc.2017.07.023 (2018).

50 Batista, V. F., Galman, J. L., G. A. Pinto, D. C., Silva, A. M. S. & Turner, N. J. *ACS Catal.* **8**, 11889-11907, doi:10.1021/acscatal.8b03525 (2018).

51 Jeon, H. *et al. Catalysts* **7**, 251, doi:10.3390/catal7090251 (2017).

52 Patil, M. D. *et al. Catalysts* **9**, 600, doi:10.3390/catal9070600 (2019).

53 Aleku, G. A. *et al. ChemCatChem* **10**, 515-519, doi:10.1002/cctc.201701484 (2018).

54 Yoon, S. *et al. ChemCatChem*, **11**, 1898-1902, doi:10.1002/cctc.201900080 (2019).

55 Geueke, B., Riebel, B. & Hummel, W. *Enzyme Microb. Technol.* **32**, 205-211, doi: 10.1016/S0141-0229(02)00290-9 (2003).

56 Knaus, T., Böhmer, W. & Mutti, F. G. *Green Chemistry* **19**, 453-463, doi:10.1039/C6GC01987K (2017).